COBEM 2023 27TH INTERNATIONAL CONGRESS OF MECHANICAL ENGINEERING

ABCM Brazilian Society of Mechanical Sciences and Engineering
27th ABCM International Congress of Mechanical Engineering
December 04-08, 2023, Florianópolis-SC, Brazil

COB-2023-0755
DETERMINATION OF THE MATERIAL REMOVAL RATE ON A-36 STEEL USING A 1064 µm NANOSECOND PULSED FIBER LASER

Santiago Javier Caraguay
Precision Engineering Laboratory, Federal University of Santa Catarina, Campus Reitor João David Ferreira Lima, s/nº, Trindade, Florianópolis - SC, CEP: 88040-900, Brazil
Instituto Senai de Inovação em Sistemas de Manufatura e Processamento a Laser, Rua Arno Waldemar Dohler, Joinville – SC, 89219-510, Brazil
santiago.correa@sc.senai.br

Thiago Soares Pereira
Francisco Ratuznei
Miriam Parra Sejas
Instituto Senai de Inovação em Sistemas de Manufatura e Processamento a Laser, Rua Arno Waldemar Dohler, Joinville – SC, 89219-510, Brazil
thiago.pereira@sc.senai.br
francisco.ratuznei@sc.senai.br
miriam.sejas@sc.senai.br

Christian Andrés Caraguay
Universidad Nacional de Loja, Facultad de la Energía, las Industrias y los Recursos Naturales no Renovables, Ciudad Universitaria Guillermo Falconí, Loja, Ecuador.
christian.caraguay@unl.edu.ec

Milton Pereira
Fabio Antônio Xavier
Precision Engineering Laboratory, Federal University of Santa Catarina, Campus Reitor João David Ferreira Lima, s/nº, Trindade, Florianópolis - SC, CEP: 88040-900, Brazil
milton.pereira@ufsc.br
f.xavier@ufsc.br

Abstract. *Laser material removal, also known as laser micromachining, is a non-contact process, with high accuracy, repeatability and flexibility, making it advantageous over other microfabrication technologies. Laser material removal rate (MRR) is determined by the interaction between the laser beam and the material. However, due to the large number of parameters that can be adjusted in the process, laser energy is often used inefficiently. The study aimed to optimize the MRR of A-36 steel using a 1064 µm nanosecond pulsed fiber laser. The overlapping between pulses, the focal position and number of pulses per laser-ablated cavity were varied to optimize the MRR. The laser-ablated cavities' profiles were measured using a stylus profilometer, and the ablation volume was determined using the average depth of the profile and the area of the cavity. The MMR was then calculated by the ratio between the volume of the removed material per pass. Scanning electron microscopy were performed to characterize the material surface after laser material removal. Results showed an increase of MRR with the increase of overlapping up to a certain limit. SEM images indicated that the parameters combinations influenced the surface morphology of the ablated cavities. Ultimately, high quality at high throughput MRR is demonstrated using optimized process parameters.*

Keywords: *Laser material removal rate, Parameters optimization, Laser micromachining.*

1. INTRODUCTION

Laser micromachining has emerged as a versatile technique for material processing, offering precise and controlled removal of material from solid surfaces (Knowles *et al.*, 2017). It finds applications in various industries, including microelectronics, biomedical engineering, and automotive manufacturing (Lopez *et al.*, 2013). Understanding the fundamental aspects of laser ablation and optimizing the process parameters are crucial for achieving desired outcomes and enhancing the efficiency of material removal (Zemaitis *et al.*, 2018).

The material removal rate (MRR) in laser micromachining is a critical factor determined by the intricate interaction between the laser beam and the targeted material. However, optimizing the efficiency of laser energy utilization remains a challenge due to the numerous adjustable parameters involved in the process (Diaci, *et al.*, 2011). Extensive research

has been conducted to investigate the effects of different parameters on laser ablation, including pulse energy, pulse duration, repetition rate, and pulse-to-pulse overlap (Petkov *et al.*, 2008). These parameters play a significant role in determining the quality and efficiency of material removal during laser processing. The understanding of their influence is vital for optimizing laser engraving processes and achieving high-quality results (Baumgratz, 2022).

During the laser material removal process, the surface of the material absorbs the energy emitted by the laser, resulting in a localized increase in temperature. When the energy surpasses the ablation threshold, which is the minimum amount of energy required for material removal through laser ablation (as defined by Liu, 1982), the material undergoes melting and/or evaporation. The ablation threshold represents the point at which the laser energy becomes adequate to break the interatomic or intermolecular bonds within the material, leading to the vaporization or expulsion of material from the surface (Dubey and Yadava, 2008). Consequently, the material experiences significant transformations such as melting, vaporization, or decomposition. However, if the laser energy falls below the ablation threshold, it is insufficient to induce these effects, and the material remains relatively unaffected.

The accumulation effect and saturation depth are phenomena which occur during laser material processing, specifically in the context of laser ablation and surface modification. The accumulation effect refers to the progressive build-up of laser energy absorption and thermal effects within a material as the laser pulses are repeatedly applied (Dondieu *et al.*, 2020). With each laser pulse, a small portion of the material is ablated or modified, resulting in changes to the material's surface. This altered surface can have different optical, thermal, and structural properties compared to the unaffected material. As subsequent laser pulses are applied, the modified surface absorbs more laser energy, leading to increased heating and further material removal or modification (Lasemi, 2018). This cumulative effect can result in enhanced material processing or improved efficiency in achieving the desired outcome, such as increased material removal rate or surface quality.

Saturation depth, on the other hand, refers to the maximum depth at which the accumulation effect becomes limited or reaches a plateau. Initially, as the laser pulses are applied, the accumulation effect leads to an increase in material removal or modification with increasing depth. However, beyond a certain depth, the material may reach a state where further accumulation of laser energy or thermal effects becomes negligible (Raciukaitis *et al.*, 2008).

This study aimed to investigate the material removal rate (MRR) of A-36 steel, which is a commonly structural steel used in industrial application. Various parameters such as pulse overlap and focal position per laser-ablated cavity were carefully adjusted in order to identify the optimal combination that would maximize the MRR. To assess the effectiveness of the laser ablation process, the profiles of the resulting cavities were measured using a stylus profilometer. Lastly, laser engraving experiments were conducted to determine the time required to remove material using the optimized parameters.

2. MATERIALS AND METHODS

Samples with dimensions of 30 mm x 20 mm x 6 mm were prepared from A-36 steel plate. The surface of the samples was sanded with SiC grit size abrasive papers, down to grit #1200. Finally, to diminish the surface roughness of the sample the surface was polished to achieve a mirror-like finish.

A nanosecond pulsed fiber laser (model SP-070P-A-EP-Z-B-Y, from SPI LASER, UK) operating at a fundamental radiation wavelength of 1064 nm was utilized for irradiate the sample surface. The laser had the capability to generate pulses with a maximum energy of 1.0 mJ and an average power of 70W. The pulse duration could be adjusted between 10 to 500 ns, while the pulse repetition rate ranged from 1 to 1000 kHz. The laser beam was delivered to the processing head through an optic system consisting of a collimator and a focusing lens. The Rayleigh length of the laser beam was about 2.5 mm. The galvanometer scanner controlled the beam position on the sample. A scheme of the experimental setup can be seen in Figure 1.

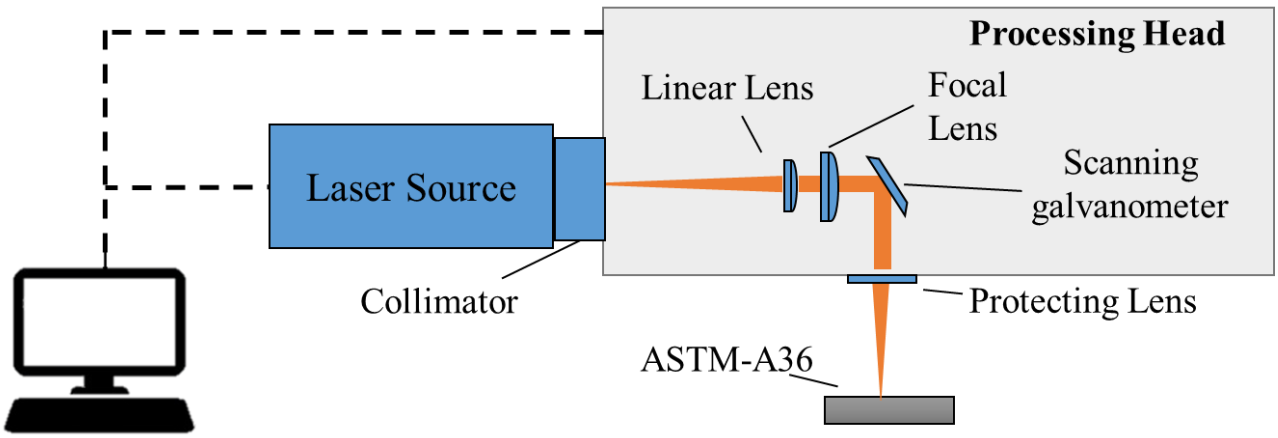

Figure 1. Schematic diagram of experimental setup.

During the irradiation process, the laser beam was focused onto the top surface of the sample. By utilizing an adjustable linear lens controlled by the processing software, the vertical position of the laser focal spot could be modified, enabling changes to the focal plane over the steel sample. The computer controlled the processing head and laser source simultaneously. The material removal rate experiments were carried out in an ambient environment.

2.1 Material removal rate experiments

The material removal rate (MMR) was calculated using the layer-by-layer approach, wherein the laser beam eliminated a specific depth of material from the substrate during each pass. To determine the MMR, the volume of the material removed in a cavity was measured for various parameter combinations. Figure 2 illustrates the experimental setup employed to determine the MRR, highlighting an array of ablated rectangular cavities and the scanning path of the laser beam. Before conducting the experiments, the surfaces of ASTM-A36 steel were cleaned using isopropyl alcohol in an ultrasonic bath.

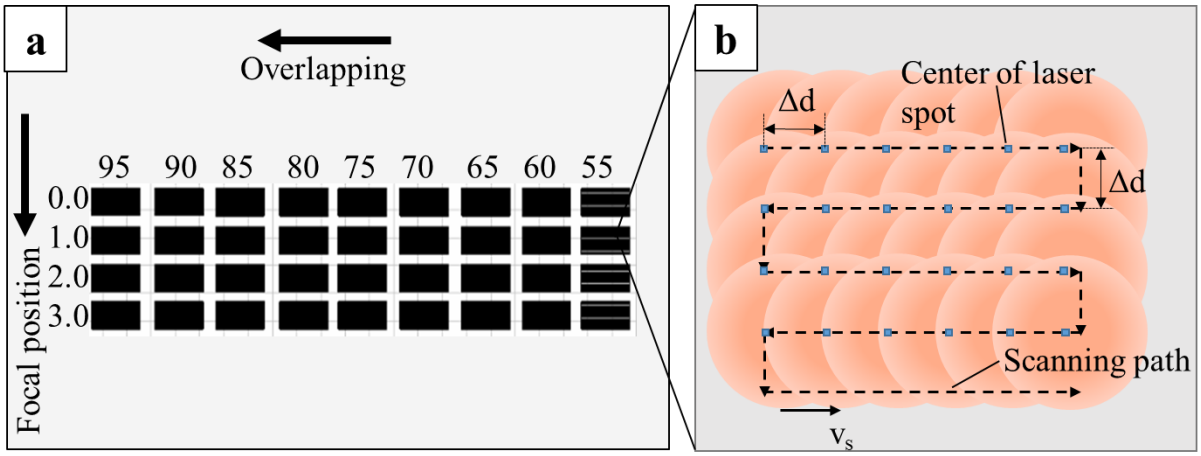

Figure 2. Experimental setup to determine the MMR, a) array of ablated rectangular cavities (tested parameters – overlapping and focal position) and, b) schematics of laser beam scanning path in each cavity.

The ablation rate measurement experiments were conducting using the highest available laser power of 70 W, with a pulse energy of 1 mJ, in order to have the maximum material removal rate (MRR). The pulse duration (at FWHM) and the pulse repetition rate was set to 46 ns and 10 kHz, respectively. The laser beam was delivered with a calculated spot diameter of around 110 µm, at the focal plane (focal position, 0.0 mm).

Figure 2.a shows the array of laser scanned rectangular areas (2.5 x 3.0 mm) on the sample with variable processing parameters. The laser processing parameters used to determine the MRR are presented in Table 1. The parameters evaluated were, the distance to the focal position, increasing from 0.0 mm at the substrate surface to 3.00 mm into the substrate surface, and overlapping, with overlapping being a result of the combination of scanning speed, pulse repetition rate and spot size.

Table 1. – Laser processing parameters used to determine the MRR.

Overlapping (%)	Scanning Speed (mm/s)	Focal Position (mm)	Number of Passes
95	55	0.0 1.0 2.0 3.0	4
90	110		15
85	165		34
80	220		60
75	275		94
70	330		135
65	385		184
60	440		240
55	495		304

The focal position corresponds to the distance from the sample surface to the focal plane situated below it. It is important to observe that as the degree of overlap decreases, the number of passes needs to increase in order to maintain an equal number of pulses per cavity. Figure 2.b demonstrates the scanning trajectory of the laser beam within each cavity. To simplify the evaluation process, the distance between the centers of laser spots (Δd) was maintained at an equal value in both the scanning direction and between adjacent lines. This approach helps minimize the number of parameters being assessed.

After conducting the experiments, the profiles of the laser-ablated cavities were measured using a stylus profilometer (Form Talysurf Limited NFTS, from Taylor Hobson). The profilometer was equipped with a diamond stylus with a tip radius of 2 µm. Figure 3.a depicts the scanning electron microscope (SEM) image, which provides a visual representation of an array of laser-ablated cavities. The figure also illustrates the scanning paths of the stylus at three different positions. In Figure 3.b, a representative profile is presented, highlighting the surface characteristics of the ablated cavity in detail. The depth of the cavity (c_d) was determined by measuring the distance between the unprocessed surface and the average line formed by the highest points and lowest points at the cavity's base.

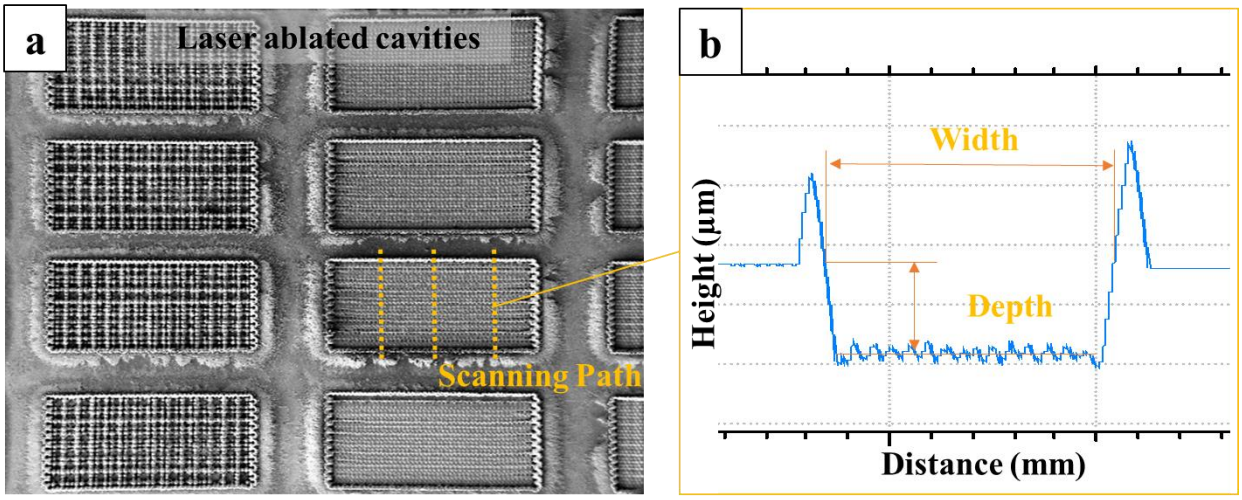

Figure 3. Laser ablated cavities, a) Scanning paths of the diamond stylus and, b) measured profile of the laser ablated cavity.

The volume of the removed material (V_c) was determined by considering both the average depth of the profile and the area of the cavities. By multiplying these characteristics of the cavities, an estimation of the volume of material could be obtained according to equation (1).

$$V_c = c_d . c_w . c_l \,, \tag{1}$$

where c_w and c_l are the cavity width and cavity length, respectively.

To determine the maximum achievable removal rate, the steel substrate was subjected to laser processing using the layer-by-layer raster scan method. The average ablated volume per single layer (V_{sl}) can be calculated using the equation (2).

$$V_{sl} = \frac{V_c}{n_p} \,, \tag{2}$$

This meticulous approach ensures a comprehensive evaluation of the material removal process, offering valuable insights into its performance.

Furthermore, the surface morphology of the ablated cavities was subjected to detailed analysis using images obtained through a Zeiss SUPRA 55VP scanning electron microscope. For this purpose, smaller samples were prepared, and cavities measuring 1.5 x 0.75 mm were fabricated. The images examination provided valuable insights into the qualitative aspects of the material removal process from the substrate.

Finally, laser engraving was performed in order to provide a tangible demonstration of the highly effective material removal achieved through this particular methodology. To further enhance the understanding of the impact of various parameters, stereoscope and microscope images were utilized to show how these factors influence the visual characteristics of the engraved text.

3. RESULTS

This study investigates the laser ablation of A-36 steel using an average laser power of 70.0 W from a nanosecond laser source and a galvanometric scanner. The laser material removal experiments were conducted using the maximum laser power to create cavities on the substrate surface. Figure 4 shows the results of the cavity depth measurements conducted using a stylus profilometer, as function of pulse-to-pulse overlap and focal position. It is apparent that the depth of the cavity progressively increases with higher overlapping values (ranging from 55% to 70%). However, beyond a certain point, further increases in overlap actually lead to a decrease in the removed depth. The observed increase can be attributed to the mechanism by which the laser beams remove material from the surface of the sample. To further support this explanation, Figure 5 presents SEM images of the ablated cavities after material removal.

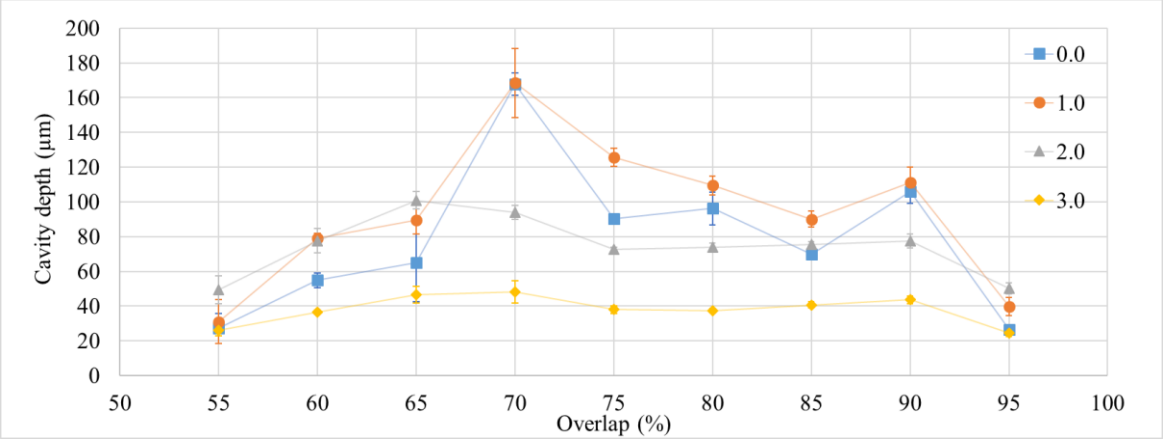

Figure 4. Depth of the laser ablated cavity after laser material removal.

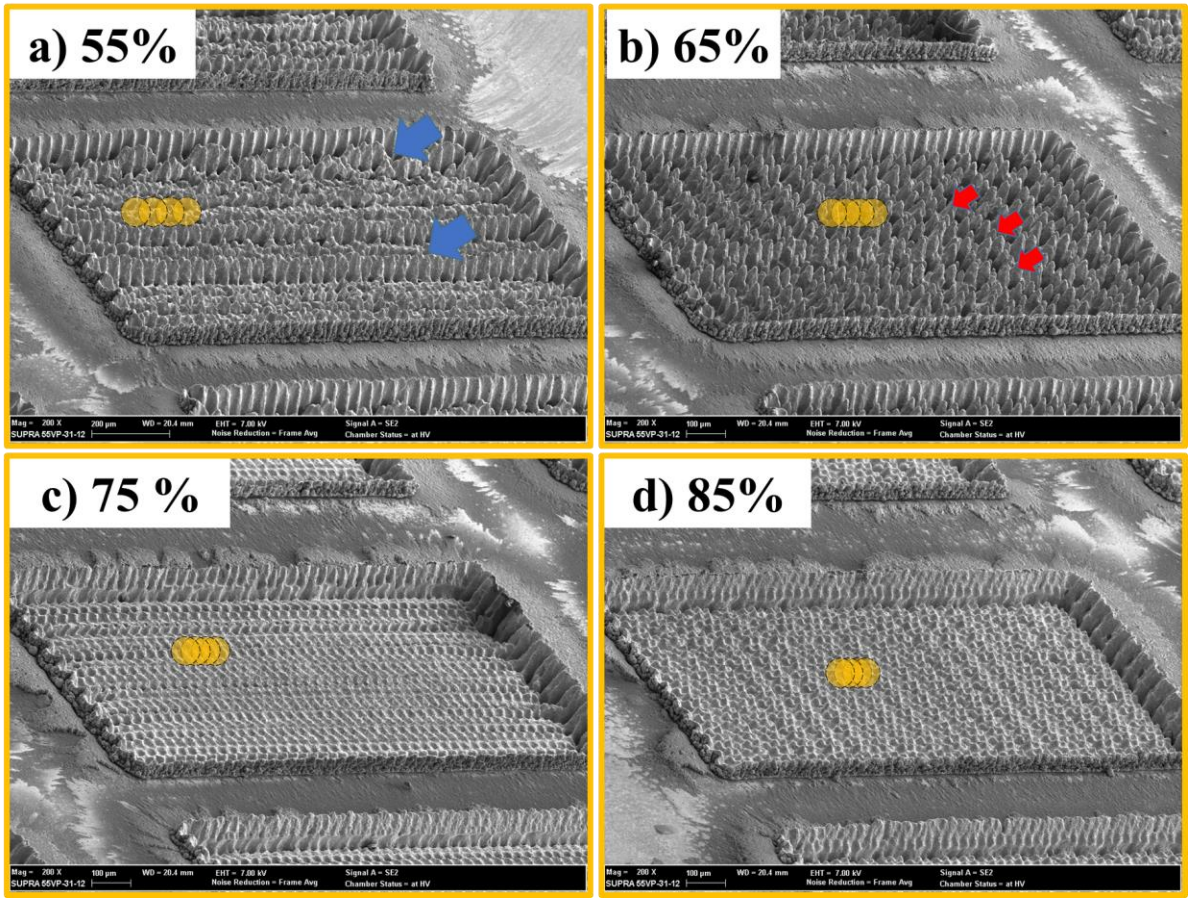

Figure 5. SEM micrographs of the laser ablated cavities at 0.0 mm focal position, with pulse-to-pulse overlap: a) 55 %, b) 65%, c) 75 %, and d) 85 %.

At an overlap of 55%, the number of laser pulses per area is relatively small due to low pulse overlap. This low overlap leads to the formation of a surface morphology characterized by clustered peaks and valleys at the bottom of the cavity, as indicated by the blue arrow in Figure 5.a. Since the depth of the cavity was measured by rastering the surface with a diamond tip, this clustered morphology results in a lower measured depth. As the overlap increases, the distance between pulses decreases, resulting in a more uniform removal of material.

In Figure 5.b, for an overlap of 65%, it can be observed that the peaks and valleys are more distinct and separated, as highlighted by the red arrows. With a further increase in overlap, the material removal becomes even more uniform, leading to higher measured depths. In addition, at this point the accumulation effect can be considered as a factor increasing the material removal. As the overlap increases, the number of pulses per area also increases. Consequently, the ablation threshold experiences a significant decrease (known as the accumulation effect), resulting in an increase in the overall depth of ablation.

To provide an explanation for the decrease in material depth, it is crucial to consider the creation of a non-uniform surface due to molten material accumulation. At an overlap of 95%, the pulse-to-pulse overlap becomes too high, causing the material to undergo a different behavior as more energy is delivered per surface area, influencing in the thermal dissipation rate on the material. Instead of ablating, the material starts to melt and resolidify on the surface. This leads to a lack of material removal and contributes to the observed low cavity depth. Decreasing the overlap, increases the quality of the material removal, causing a better material removal, with a better thermal management.

The depth of material removal was found to be highest for focal positions of 0.00 mm and 1.00 mm, while the least amount of material was removed at 2.00 mm and 3.00 mm focal positions. Notably, the 1.00 mm focal position below the surface consistently resulted in the greatest depths across most conditions. When the laser starts removing material, subsequent passes begin at positions higher than the processed sample surface. If the focal position is below the surface, as material is removed, the energy increases, leading to more efficient material removal. This phenomenon occurs when the energy is sufficiently high to effectively remove material, but it is not observed at the focal positions of 2.00 mm and 3.00 mm. Considering the calculated Rayleigh length of the laser beam, which is approximately 2.5 mm, it can be inferred that the energy starts to diminish above this length. Although the 2.00 mm focal position falls within this length, the propagation of the laser beam can introduce additional effects on energy distribution, altering the material removal process. Above this Rayleigh length, there are larger laser spot sizes with lower energy density, making it challenging to achieve fluence above the ablation threshold, resulting in low ablation depths. These focal positions yield low to moderate ablation rates for the conditions tested.

Figure 6.a illustrates the volume of material removed per single layer as a function of pulse-to-pulse overlap. The results demonstrate that increasing the overlap leads to an increase in the removed volume (V_{sl}). It is noteworthy that the material removal is more effective for the focal points at 0.00 mm and 1.00 mm, with the exception of a 95% overlap. This behavior is likely caused by the phenomenon of saturation of ablation depth during multi-pulse irradiation. As the distance between pulses increases, there comes a point of saturation where the ablation depth no longer continues to increase because of the local thermal management. At this saturation point, the ablation rate reaches moderate values and subsequently decreases as the pulse-to-pulse overlap continues to increase. For the 2.00 mm and 3.00 mm focal points, the fluence is lower, and the saturation effect has a lower impact. Consequently, there is a better removal of material observed in these cases.

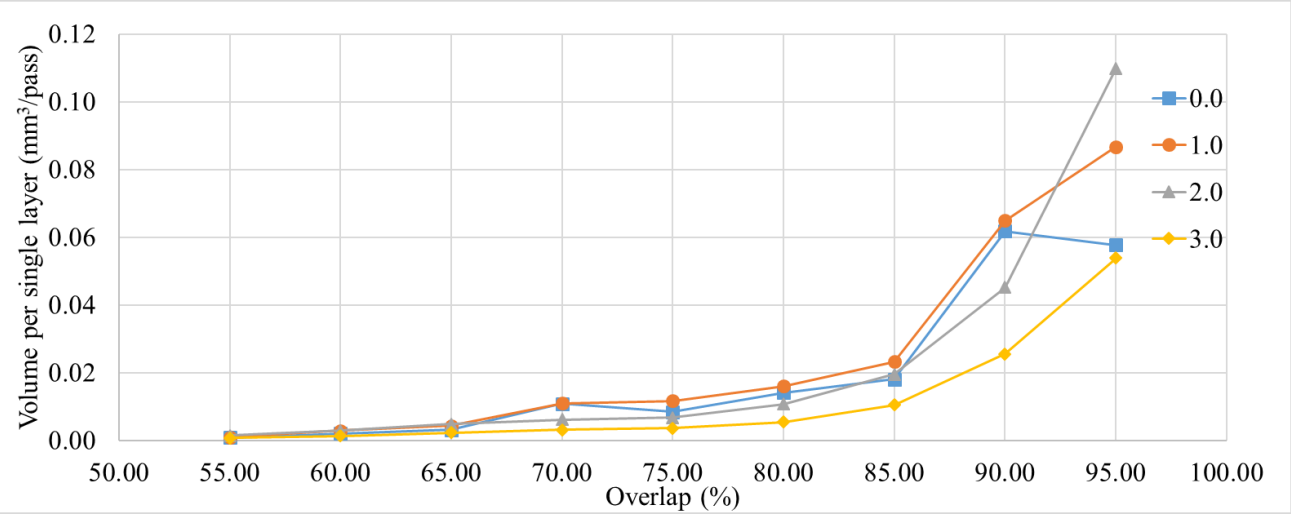

Figure 6. Volume of material removed per single layer as function of pulse-to-pulse overlap.

One of the primary objectives of this study was to demonstrate the capability of the methodology employed to optimize laser processing parameters for laser engraving. To achieve this, the text "SENAI" was engraved on a steel substrate, with each letter being engraved using different process parameters. Specifically, the letters S, E, N, A, and I

were processed with pulse-to-pulse overlaps of 95%, 85%, 75%, 65%, and 55%, respectively. The number of passes were the same as the ones presented in Table 1. The focal position was 1.0 mm below the surface.

In Figure 7.a the laser-engraved text is depicted immediately after the laser processing. The samples present oxides at the borders of the letters. It is worth noting that the letter S appears darker, indicating excessive heat generation at a 95% overlap. By reducing the overlap, a more uniform energy distribution on the sample surface and improved material removal can be observed, as demonstrated by the better quality of the letter N. In contrast to the letter S, the dark coloration on letters A and I is attributed to light refraction caused by the surface morphology at the bottom of these letters.

In order to remove the oxidation, a laser-cleaning process was performed with the same laser system. A pulse energy of 0.08 mJ, a pulse duration of 9 ns and a pulse repetition rate of 10 kHz were used. The scan speed was set to 380 mm.s-1. After cleaning the sample, the quality of the engraved text becomes more evident, as shown in Figure 7.b. The decrease in pulse-to-pulse overlap becomes more noticeable within the letters, particularly for letters A and I, where the decreased overlap is apparent. This effect is also visible at Figure 7.c, where optical microscope images display magnified views of the surfaces within the letters. It is important to note that the microscope was intentionally defocused to enhance the visualization of the engraving depth. The largest depth measurement was observed in the letter N, which correlates well with the results presented in Figure 4.

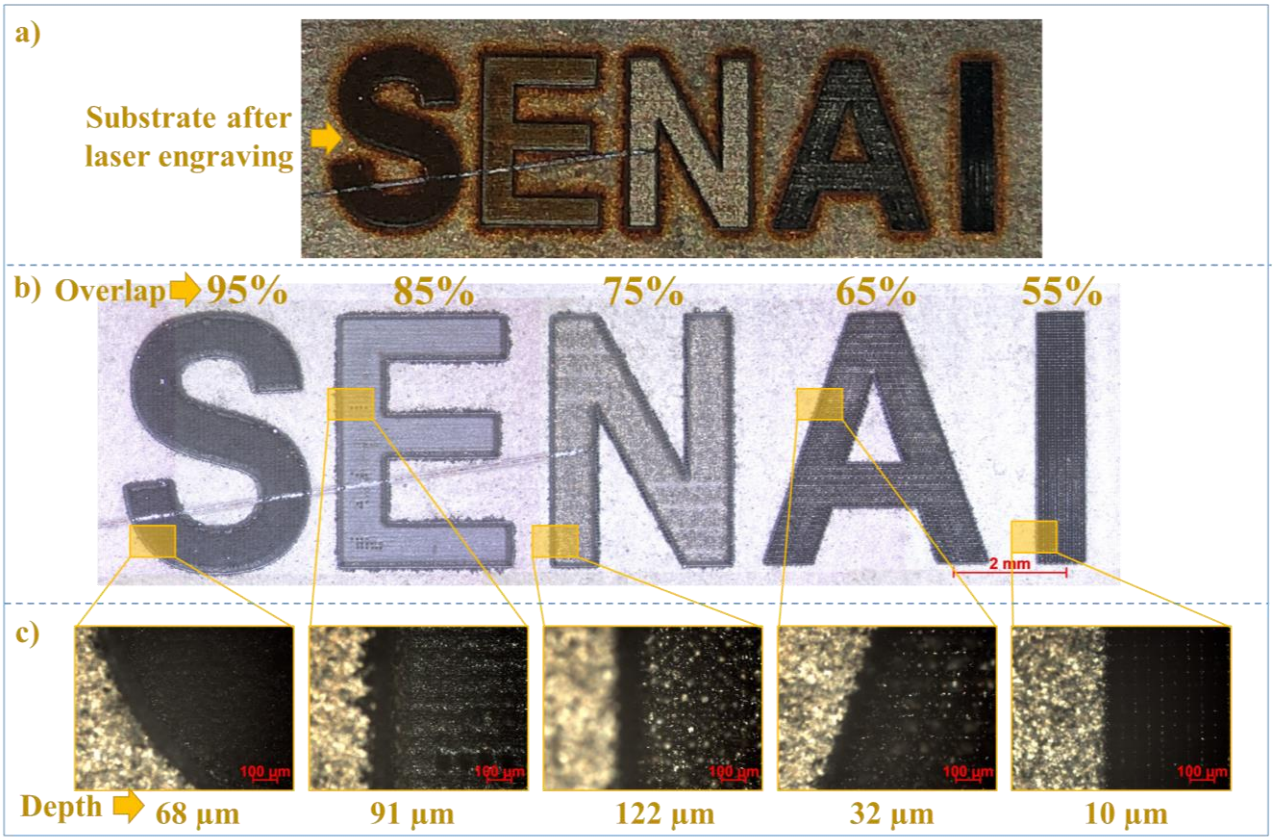

Figure 7. Results of laser surface engraving the text “SENAI” on A-36 steel: a) the sample after laser processing, b) a stereoscopic image of the text after laser cleaning, and c) optical microscope images of different regions with their corresponding depths. Laser processing parameters: wavelength of irradiation 1064 nm; mean laser power 70.0 W; pulse repetition rate 10 kHz; pulse duration 46 ns.

Finally, an engraved sample depicted in Figure 8 served as the basis for determining the material removal rate associated with a 75% overlap. Through careful examination, the depth of the engraved letters was estimated to be approximately 0.122 mm, according to the results shown in Figure 7.c (overlap of 75%). Through the Image J software, the processed area was estimated in order to obtain an estimated value of removal rate. Figure 8 illustrates the measurement of the “L” letter in the engraved text as an example, but it´s important to note that the measurement was conducted for the entire text. The resulting total area was about of 69.81 mm^2. Therefore, a significant amount of material of about 8,5 mm^3 was effectively removed. The process of engraving this text required a duration of 8.9 minutes, through calculations a material removal rate of approximately 0.96 mm^3 per minute. By incorporating 3D measurements, a more appropriate calculation of the removed material can be obtained, enabling the acquisition of precise and accurate data regarding the amount of material that has been removed.

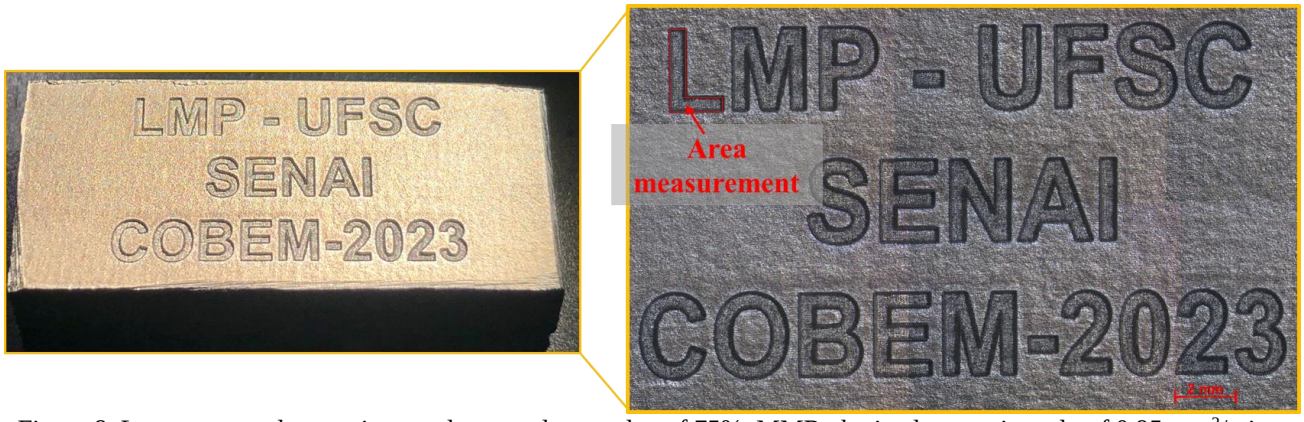

Figure 8. Laser engraved text using a pulse-to-pulse overlap of 75%. MMR obtained approximately of 0,95 mm^3/min.

It is noteworthy that the achieved material removal rate (MMR) can be further enhanced by increasing the pulse repetition rate, which in turn allows for higher scanning speeds, if the laser source is adequate to work in higher nominal repetition rates. Existing literature reports of MMR values ranging from approximately 10 to 12 mm^3/min for a pulse repetition rate of 100 kHz (Dondieu *et al.* 2020), which can be considered comparable to our results obtained at 10 kHz. This suggests that there is potential to attain similar MMR levels by utilizing higher pulse repetition rates, thus warranting further exploration and investigation.

4. CONCLUSION

This study investigated the laser ablation of A-36 steel using a nanosecond laser source and a galvanometric scanner. The results revealed that the depth of the laser ablated cavities progressively increased with higher pulse-to-pulse overlaps, ranging from 55% to 70%. However, beyond a certain point, further increases in overlap led to a decrease in the removed depth. SEM images of the ablated cavities confirmed the observations, showing distinct surface morphologies at different pulse-to-pulse overlaps. At an overlap of 55%, the low pulse overlap resulted in a clustered morphology with peaks and valleys at the bottom of the cavity. As the overlap increased, the material removal became more uniform, and the peaks and valleys became more separated. The focal position also influenced the material removal, with the depths being highest at focal positions of 0.00 mm and 1.00 mm below the surface. This is attributed to the energy increase as the laser removes material from a position below the surface, leading to more efficient material removal. In contrast, at focal positions of 2.00 mm and 3.00 mm, the larger spot sizes resulted in lower energy per cm^2 made it difficult to achieve fluence above the ablation threshold, resulting in lower ablation depths.

In order to enhance this methodology, the utilization of 3D scanning systems can be employed to achieve a higher level of accuracy in measuring the removed volume. By doing so, errors resulting from 2D measurements can be minimized, as variations in peaks and valleys can lead to inconsistent profile depths of the cavities.

Overall, this study provided valuable insights into the laser ablation of A-36 steel and the optimization of laser engraving parameters. The findings contribute to the understanding of the relationship between pulse-to-pulse overlap, focal position, and material removal, enabling the development of more efficient laser processing techniques. The outcomes of this study facilitates the development of more precise and efficient fabrication methods for various applications requiring intricate material removal.

5. ACKNOWLEDGEMENTS

The authors gratefully acknowledge to the Instituto Senai de Inovação em Sistemas de Manufatura e Processamento a Laser and to National Council for Scientific and Technological Development (CNPq) for the assistance provided for the development of this work.

6. REFERENCES

Baumgratz, F.M., 2022. *Three-dimensional laser beam micro-machining: methodology, development and implementation*. Master's thesis, Graduate Program in Mechanical Engineering, Federal University of Santa Catarina, Florianópolis, Brasil.

Diaci, J., Braun, D., Gorki, A., Moina, J., 2011 "Rapid and flexible laser marking and engraving of tilted and curved surfaces". *Optics and Lasers in Engineering*. Vol. 49, pp. 195–199.

Dondieu, S.D., Wlodarczyk, K.L., Harrison, P., Rosowski, A., Gabzdyl, J., Reuben, R.L., Hand, D.P. 2020. "Process Optimization for 100 W Nanosecond Pulsed Fiber Laser Engraving of 316L Grade Stainless Steel." *Journal of Manufacturing Material Processes*. Vol,4. pp, 110.

Dubey, A.K., Yadava V. 2008. “Laser beam machining - A review”. *International Journal of Machine Tools and Manufacture*. Vol. 48, n. 6, pp. 609–28.

Knowles, M.R.H., Rutterford, G., Karnakis, D., Ferguson, A. 2007. “Micro-machining of metals, ceramics and polymers using nanosecond lasers”. *International Journal of Advanced Manufacturing Technology*. Vol. 33, pp. 95 – 102.

Lasemi, N., Pacher, U., Zhigilei, L.V., Bomatí-Miguel, O., Lahoz, R., Kautek, W., 2018. “Pulsed laser ablation and incubation of nickel, iron and tungsten in liquids and air”. *Applied Surface Science*, Vol. 433, pp. 772-779.

Liu, J.M. 1982. “Simple Technique for measurements of pulsed Gaussian-beam spot sizes”. *Optics Letters*, Vol. 7. pp. 196-198.

Lopez, J., Zaouter, Y., Torres, R., Faucon, M., Hönninger, C., Georges, P., Kling, R. 2013. “Parameters of influence in surface ablation of metals with using a high power tunable ultrafast laser”. *In Proceedings of the ICALEO 2013—32nd International Congress on Applications of Lasers and Electro-Optics*, Miami, FL, USA.

Petkov, P.V.; Dimov, S.S.; Minev, R.M.; Pham, D.T. 2008. “Laser milling: Pulse duration effects on surface integrity”. *Proceedings of the Institution of Mechanical Engineers Part B Journal of Engineering Manufacture*, Vol. 222, pp. 35–45.

Raciukaitis, G., Brikas, M., Gecys, P., Gedvilas, M. 2008 “Accumulation effects in laser ablation of metals with high-repetition-rate lasers", *Proc. SPIE 7005, High-Power Laser Ablation VII*, 70052L.

Žemaitis, A., Gaidys, M., Brikas, M., Gecys, P., Raciukaitis, G., Gedvilas, M. 2018 “Advanced laser scanning for highly-efficient ablation and ultrafast surface structuring: experiment and model”. *Scientifics Reports*, pp 17376.

7. RESPONSIBILITY NOTICE

The authors are the only responsible for the printed material included in this paper.